

Asymmetric Ferromagnetic Criticality in Pyrochlore Ferromagnet $\text{Lu}_2\text{V}_2\text{O}_7$

N. Su^{1,6,*}, F. -Y. Li^{2,*}, Y. Y. Jiao^{1,6,†}, Z. Y. Liu^{1,3}, J. P. Sun^{1,6}, B. S.

Wang^{1,6,7}, Y. Sui³, H. D. Zhou⁴, G. Chen^{2,5,‡}, and J. -G. Cheng^{1,6,7,§}

¹*Beijing National Laboratory for Condensed Matter Physics and Institute of Physics,
Chinese Academy of Sciences, Beijing 100190, China*

²*State Key Laboratory of Surface Physics and Department of Physics, Fudan University, Shanghai 200433, China*

³*Department of Physics, Harbin Institute of Technology, Harbin 150001, China*

⁴*Department of Physics and Astronomy, University of Tennessee, Knoxville, TN 37996, USA*

⁵*Department of Physics and Center of Theoretical and Computational Physics,
The University of Hong Kong, Pokfulam Road, Hong Kong, China*

⁶*School of Physical Sciences, University of Chinese Academy of Sciences, Beijing 100190, China*

⁷*Songshan Lake Materials Laboratory, Dongguan, Guangdong 523808, China*

(Dated: March 11, 2022)

Critical phenomenon at the phase transition reveals the universal and long-distance properties of the criticality. We study the ferromagnetic criticality of the pyrochlore magnet $\text{Lu}_2\text{V}_2\text{O}_7$ at the ferromagnetic transition $T_c \approx 70$ K from the isotherms of magnetization $M(H)$ via an iteration process and the Kouvel-Fisher method. The critical exponents associated with the transition are determined as $\beta = 0.32(1)$, $\gamma = 1.41(1)$, and $\delta = 5.38$. The validity of these critical exponents is further verified by scaling all the $M(H)$ data in the vicinity of T_c onto two universal curves in the plot of $M/|\varepsilon|^\beta$ versus $H/|\varepsilon|^{\beta+\gamma}$, where $\varepsilon = T/T_c - 1$. The obtained β and γ values show asymmetric behaviors on the $T < T_c$ and the $T > T_c$ sides, and are consistent with the predicted values of 3D Ising and cubic universality classes, respectively. This makes $\text{Lu}_2\text{V}_2\text{O}_7$ a rare example in which the critical behaviors associated with a ferromagnetic transition belong to different universality classes. We describe the observed criticality from the Ginzburg-Landau theory with the quartic cubic anisotropy that microscopically originates from the anti-symmetric Dzyaloshinskii-Moriya interaction as revealed by recent magnon thermal Hall effect and theoretical investigations.

As a representative subject of quantum magnetism, pyrochlore antiferromagnets have attracted a significant attention in recent years [1]. Many interesting phenomena including classical spin ice [2, 3], quantum spin ice [4–6], pyrochlore ice U(1) spin liquid [5, 7–10], quantum order by disorder [11, 12], spin nematics [13, 14], symmetry enriched topological orders [10, 15, 16], topological magnetic excitations [17–19] have been proposed and/or discovered for various compounds in the pyrochlore antiferromagnet families. While most efforts of this field have been devoted to the antiferromagnets, the pyrochlore ferromagnet $\text{Lu}_2\text{V}_2\text{O}_7$ may stand out in the field of pyrochlore magnets by providing some rather unique and robust phenomena [20–25]. $\text{Lu}_2\text{V}_2\text{O}_7$ is a vanadium based pyrochlore Mott insulator that orders ferromagnetically below about 70 K. Although it is a conventional ferromagnet, this material shows a remarkable magnon thermal Hall transport under magnetic field. Microscopically, the large thermal Hall effect [24, 25] in this material is attributed to the non-trivial Berry curvature of the thermally populated magnon bands that originate from the antisymmetric Dzyaloshinskii-Moriya (DM) interaction [24–27] between the V^{4+} spin-1/2 localized moments on the pyrochlore lattice. Since this discovery, $\text{Lu}_2\text{V}_2\text{O}_7$ has become one of the stereotypes for the thermal Hall transports in Mott insulating materials.

To motivate our work, we here provide a general discussion about the magnetic properties of the pyrochlore ferromagnet $\text{Lu}_2\text{V}_2\text{O}_7$ or any conventionally ordered mat-

ter. For the conventional ordered states, there are several basic and phenomenological aspects. The first one would be the order parameter and the ordering structure. $\text{Lu}_2\text{V}_2\text{O}_7$ is a conventional ferromagnet. Being a ferromagnet is a global static property, the system should have a non-collinear spin structure within the four-sublattice unit cell. This is a direct consequence of the DM interaction. The second one would be the dynamic property or fluctuation with respect to the magnetic order. The thermal Hall transport is an overall effect caused by the magnetic excitations and reflects the weighted average of the Berry curvatures over the magnon bands [24, 25]. More detailed information about the dynamics would come from the magnon dispersion directly. This could be obtained through inelastic neutron scattering measurements. Theoretically, it has been suggested that the Weyl magnons [17] may be present from studying a minimal model for $\text{Lu}_2\text{V}_2\text{O}_7$ and can be one origin for the thermal Hall effect in this system [28, 29]. The third aspect is the critical property due to the fluctuations of order parameters associated with this ferromagnetic transition in $\text{Lu}_2\text{V}_2\text{O}_7$. This aspect has not been carefully considered. Given the growing interests in this simple ferromagnetic pyrochlore oxide, we are motivated to explore its critical behaviors around T_c via analyzing the isotherms of magnetization $M(H)$ with an iteration process and the Kouvel-Fisher method. Remarkably, we find that the critical exponents on both sides of T_c are not equal and show 3D Ising-like and 3D cubic-like universality classes

on each side. This differs from the conventional wisdom about the criticality that the asymmetry usually occurs in the non-universal prefactors of the scaling law rather than the scaling exponents. We discuss this asymmetric ferromagnetic criticality within Ginzburg-Landau theory and provide our view on the microscopic properties of the V-based pyrochlore magnet $\text{Lu}_2\text{V}_2\text{O}_7$. We further give a general comment about the spin-orbit coupling and the Kitaev physics in the V-based magnets.

The critical behaviors of $\text{Lu}_2\text{V}_2\text{O}_7$ around the ferromagnetic transition can be described by a series of critical exponents β , γ , and δ that reflect the effective magnetic interactions at play [30]. Different critical exponents have been derived theoretically for different models, *e.g.* $\beta = 0.365$ and $\gamma = 1.386$ for 3D Heisenberg model, $\beta = 0.345$ and $\gamma = 1.316$ for 3D XY model, and $\beta = 0.325$ and $\gamma = 1.24$ for 3D Ising model, respectively [31]. These exponents are obtained by analyzing the isothermal magnetizations $M(H)$ near T_c , *viz.*

$$M_s(T) \propto (T_c - T)^\beta \quad \text{for } T < T_c, \quad (1)$$

$$\chi_0^{-1}(T) \propto (T - T_c)^\gamma \quad \text{for } T > T_c, \quad (2)$$

$$M(H) \propto H^{1/\delta} \quad \text{for } T = T_c, \quad (3)$$

where M_s is the spontaneous magnetization and χ_0^{-1} is the inverse initial magnetic susceptibility, respectively. In a previous work, Zhou *et al.* [32] have obtained the critical exponents $\beta = 0.42$ and $\gamma = 1.85$ for $\text{Lu}_2\text{V}_2\text{O}_7$ and ascribed them to a 3D Heisenberg model. However, these values show a large deviation from those predicted theoretically. In addition, the straight lines in the modified Arrott plot, $M^{1/\beta}$ versus $(H/M)^{1/\gamma}$, are not parallel at all. Here, we reinvestigate its critical behaviors around T_c via analyzing the isotherms of magnetization $M(H)$ with an iteration process and the Kouvel-Fisher method. Interestingly, we found that the obtained $\beta = 0.322$ at $T < T_c$ and $\gamma = 1.41$ at $T > T_c$ are close to the predicted values of 3D Ising and 3D Heisenberg or cubic universality classes, respectively. $\text{Lu}_2\text{V}_2\text{O}_7$ single crystals used in the present study were grown with the traveling-solvent floating-zone technique. Details about the crystal growth and sample characterizations have been published elsewhere [32]. The magnetic properties of $\text{Lu}_2\text{V}_2\text{O}_7$ were measured with a commercial Magnetic Property Measurement System (MPMS-III, Quantum Design).

In Fig. 1(a), we plot the temperature dependence of dc magnetic susceptibility $\chi(T)$ and its inverse $\chi^{-1}(T)$ measured under $\mu_0 H = 0.1$ T in both zero-field-cooled (ZFC) and field-cooled (FC) modes. As can be seen, the ZFC and FC $\chi(T)$ curves are overlapped with each other and the ferromagnetic transition around $T_c \approx 70$ K can be clearly visible from the sharp rise of $\chi(T)$. In the paramagnetic region above T_c , we have applied the Curie-Weiss (CW) fitting to $\chi^{-1}(T)$ in the temperature range 150-300 K and extracted the effective moment of $\mu_{\text{eff}} = 1.89 \mu_B/V^{4+}$ and the Weiss temperature

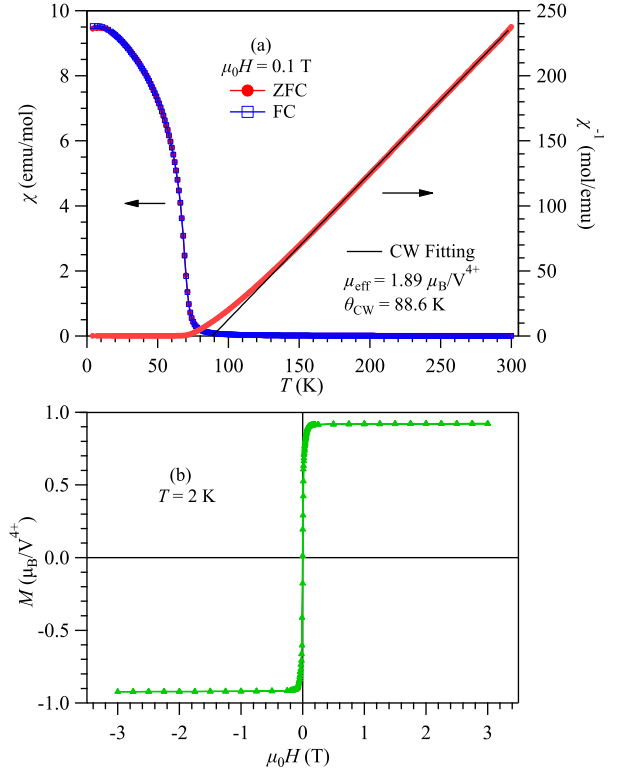


FIG. 1. (Color online.) (a) Temperature dependence of dc magnetic susceptibility $\chi(T)$ and its inverse $\chi^{-1}(T)$ measured in both zero-field-cooled (ZFC) and field-cooled (FC) modes under $\mu_0 H = 0.1$ T. The solid line is the Curie-Weiss (CW) fitting curve. (b) Isothermal magnetization $M(H)$ curve at 2 K.

$\theta_{\text{CW}} = 88.6$ K. The obtained μ_{eff} is closed to expected value of $1.73 \mu_B$ for $S = 1/2$ of V^{4+} , and the deviation from this ideal value originates from the spin-orbit coupling of the V^{4+} ion. The positive θ_{CW} signals the dominant ferromagnetic exchange interactions in this system. Fig. 1(b) displays the $M(H)$ curve at 2 K, which exhibits a typical ferromagnetic behavior and reaches a saturation moment of $\sim 1.0 \mu_B$ as expected. All these results are consistent with those reported previously and confirm the high quality of the studied crystal [32].

In Fig. 2(a), we plot the isothermal $M(H)$ curves of $\text{Lu}_2\text{V}_2\text{O}_7$ in the temperature range of 60-80 K, which covers the ferromagnetic transition. The demagnetization effect has been corrected. These $M(H)$ data are replotted in the Arrott plot M^2 vs H/M in Fig. 2(b), and in the modified Arrott plots $M^{1/\beta}$ vs $(H/M)^{1/\gamma}$ with the critical exponents of 3D Heisenberg and 3D Ising models in Fig. 2(c) and (d), respectively. The curved Arrott plot in Fig. 2(b) rules out the possibility of mean-field model, but the positive slope of the M^2 vs H/M confirms that the paramagnet-ferromagnet transition is a continuous transition. On the other hand, the modified Arrott plots in Fig. 2(c) and (d) gave roughly parallel straight lines,

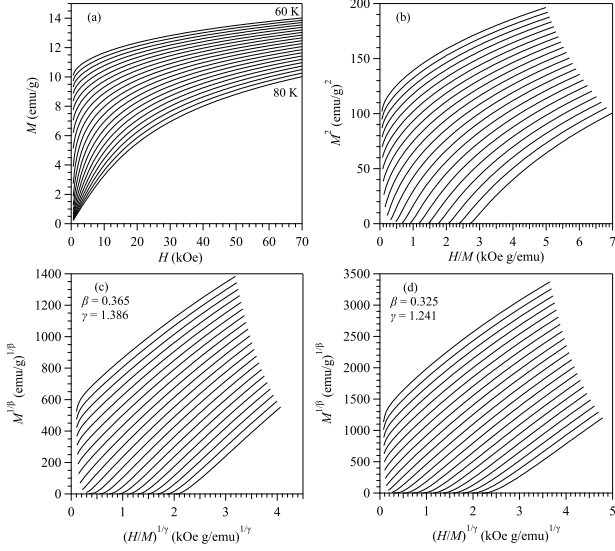


FIG. 2. (Color online.) (a) Isothermal magnetization curves between 60 and 80 K, and the modified Arrott plots of these curves with critical exponents of (b) mean field model $\beta = 0.5$, $\gamma = 1$, (c) 3D Heisenberg model $\beta = 0.365$, $\gamma = 1.386$, (d) 3D Ising model $\beta = 0.325$, $\gamma = 1.241$.

and it is hard to distinguish visually which model could better describe the ferromagnetism of $\text{Lu}_2\text{V}_2\text{O}_7$.

In order to determine precisely the critical exponents, we employed an iteration process in analyzing the isothermal $M(H)$ data near T_c based on the general formula (1) to (3) given above [33, 34]. Starting from the Arrott plot shown in Fig. 2(b), we obtain the first set of $M_s(T)$ and $\chi_0^{-1}(T)$ by extrapolating the corresponding M^2 vs H/M curves to the vertical and horizontal axes, respectively. As shown in Fig. 3(a), the obtained $M_s(T)$ and $\chi_0^{-1}(T)$ are fitted with the Eqs. (1) and (2), respectively, to extract the first set of critical exponents and critical temperatures, i.e. $\beta = 0.414(6)$, $T_c^- = 71.38(3)$ K, and $\gamma = 1.34(5)$, $T_c^+ = 69.2(3)$ K as listed in the figure. By using the obtained β and γ values, we then construct a modified Arrott plot $M^{1/\beta}$ vs $(H/M)^{1/\gamma}$ and repeat the above process to obtain the second set of $M_s(T)$ and $\chi_0^{-1}(T)$ and the corresponding critical exponents and critical temperatures. As illustrated in Fig. 3(a), after three iterations the fitting parameters are converged to $\beta = 0.322(1)$, $T_c^- = 67.91(1)$ K, and $\gamma = 1.402(3)$, $T_c^+ = 67.7(1)$ K. These critical exponents are different from those reported previously [32].

We further determine the critical exponents by employing the Kouvel-Fisher relation [35], *viz.*

$$M_s(T)[dM_s/dT]^{-1} = \frac{T - T_c^-}{\beta}, \quad (4)$$

$$\chi_0^{-1}(T)[d\chi_0^{-1}/dT]^{-1} = \frac{T - T_c^+}{\gamma}, \quad (5)$$

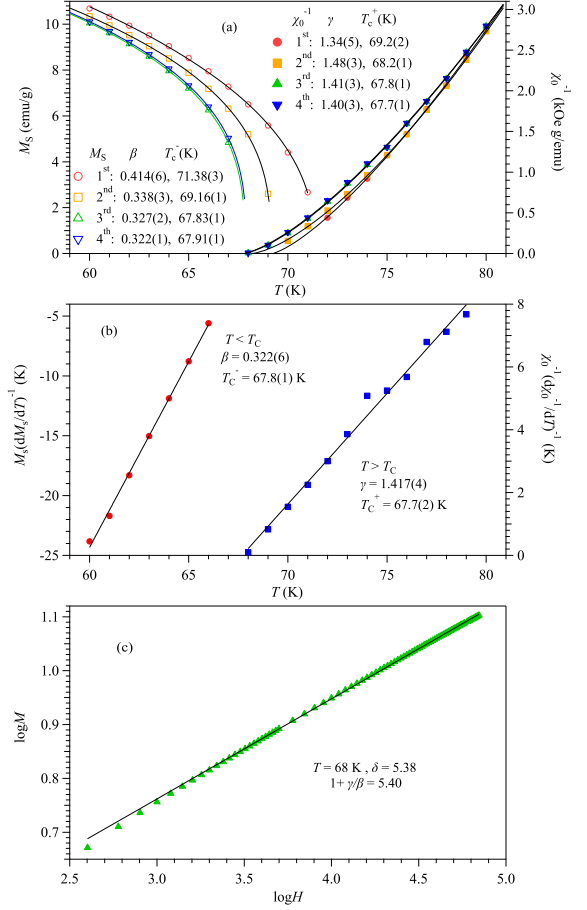


FIG. 3. (Color online.) Critical exponents β and γ , and critical temperatures T_c^- and T_c^+ determined from (a) an iteration process started from the mean-field Arrott plot, and (b) Kouvel-Fisher plots. (c) Critical isotherm at $T = 68$ K in a double logarithmic plot and a linear fitting to extract the critical exponent δ . The Widom scaling relation, $\delta = 1 + \gamma/\beta$.

in which the $M_s(T)$ and $\chi_0^{-1}(T)$ were obtained from the modified Arrott plot with the final critical exponents obtained above. As shown in Fig. 3(b), linear fittings to the plots of $M_s[dM_s/dT]^{-1}$ and $\chi_0^{-1}[d\chi_0^{-1}/dT]^{-1}$ versus T yield $\beta = 0.322(6)$, $T_c^- = 67.8(1)$ K, and $\gamma = 1.417(4)$, $T_c^+ = 67.7(2)$ K. Both values of β and γ obtained by the Kouvel-Fisher relation agree well with results from the iterations of modified Arrott plot, confirming the validity of these above analysis. For the completeness, we also estimate the critical exponent δ . In Fig. 3(c), we display the double logarithmic plot of M vs H at 68 K, which is very close to the critical temperature $T_c = 67.8(1)$ K determined above. As can be seen, the data falls nearly on a straight line with a slope of $1/\delta$ according to Eq. (3), and a linear fitting to the data at high-field region gives $\delta = 5.38$, which fulfills the Widom scaling relation perfectly [36], *i.e.* $\delta = 1 + \gamma/\beta$ by using $\gamma = 1.417$ and $\beta = 0.322$ obtained above.

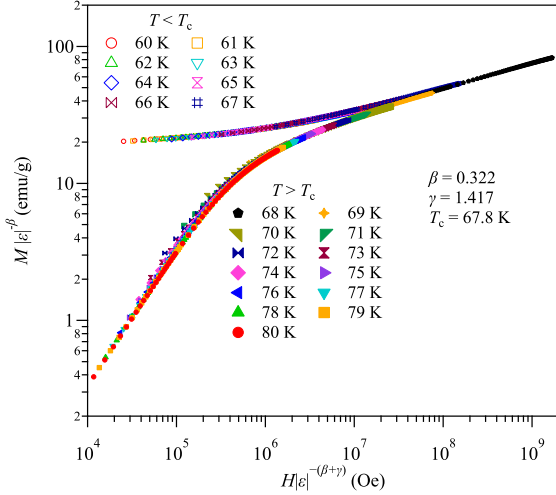


FIG. 4. (Color online.) Scaling plot for $\text{Lu}_2\text{V}_2\text{O}_7$ below and above T_c based on the critical temperature $T_c = 67.8$ K and $\beta = 0.322$ and $\gamma = 1.417$.

To check the reliability of our analysis on the critical behavior of $\text{Lu}_2\text{V}_2\text{O}_7$, we test the obtained critical exponents according to the prediction of the scaling hypothesis [30]. In the critical asymptotic region, the magnetic equation of state could be expressed as

$$M(H, \varepsilon) = |\varepsilon|^\beta f_\pm(H/|\varepsilon|^{\beta+\gamma}), \quad (6)$$

where f_+ for $T > T_c$ and f_- for $T < T_c$ are regular analytical functions, and $\varepsilon = T/T_c - 1$ is the reduced temperature. Eq. (6) implies that for the right choice of β , γ , and δ values, $M/|\varepsilon|^\beta$ as a function of $H/|\varepsilon|^{\beta+\gamma}$ should produce two universal curves: one for $T > T_c$ and the other for $T < T_c$. By using the values of β and γ obtained by the Kouvel-Fisher method and $T_c = 67.8$ K, we have obtained the scaling plot shown in Fig. 4. It is clearly seen that all the points indeed collapse into two separate branches. These well-scaled curves in Fig. 4 thus further confirm the reliability of the obtained critical exponents.

We have listed the critical exponents of $\text{Lu}_2\text{V}_2\text{O}_7$ in Table I and compared with those of ferromagnetic perovskite YTiO_3 [37] as well as the theoretical values from different models [31, 38]. Firstly, we found that the critical exponents for these two ferromagnetic oxides with $S = 1/2$ are stunningly similar with each other. Secondly, it is interesting to note that their β and γ values are not consistent with those predicted by a single model. Instead, β is very close to the predicted value of 3D Ising universality class, whereas γ is close to the predicated value of 3D Heisenberg or cubic universality class. This makes $\text{Lu}_2\text{V}_2\text{O}_7$ and YTiO_3 rather rare cases in which the critical behaviors above and below T_c are described by two different universality classes. This finding is intriguing because the critical behavior associated with a continuous phase transition should be described by one

universality class with a single set of critical exponents, and the asymmetric behaviors usually occur in the non-universal prefactors of the scaling relations. The transition from the 3D Heisenberg/cubic to Ising universality class across T_c implies the reduction of spin dimensionality or effective spin components upon the ferromagnetic ordering. As mentioned above, recent experimental and theoretical investigations on $\text{Lu}_2\text{V}_2\text{O}_7$ have revealed the presence of significant anisotropic interactions in the form of DM interaction [24–27], which should be responsible for such a transition.

	β	γ	δ	Ref.
$\text{Lu}_2\text{V}_2\text{O}_7$	0.322	1.402	5.38	This work
YTiO_3	0.328	1.441	5.39	[37]
3D Ising	0.325	1.241	4.82	[31]
3D XY	0.345	1.316	4.81	[31]
3D Heisenberg	0.365	1.386	4.8	[31]
3D Cubic	0.364	1.390	4.82	[38]

TABLE I. Critical exponents of the single-valent $S = 1/2$ ferromagnetic oxides, $\text{Lu}_2\text{V}_2\text{O}_7$ with the pyrochlore structure and YTiO_3 with the perovskite structure, in comparison with the theoretical values from different models.

The observation of similar critical behaviors in $\text{Lu}_2\text{V}_2\text{O}_7$ and YTiO_3 is not completely unexpected since both V^{4+} and Ti^{3+} ions have identical $3d^1$ electronic configuration with an active orbital degree of freedom in the octahedrally coordinated environments. The active orbitals are the lower t_{2g} orbitals for both compounds. For $\text{Lu}_2\text{V}_2\text{O}_7$, we know that the trigonal distortion would further split the t_{2g} orbitals into a_{1g} orbital and e'_{2g} orbitals. On the other hand, the atomic spin-orbit coupling is active for the t_{2g} orbitals. The spin-1/2 local moment of the V^{4+} ion should be interpreted as the effective spin-1/2 of the ground state Kramers doublet for a local single-ion Hamiltonian with the spin-orbit coupling and the trigonal distortion. From this perspective, the nature of the V^{4+} local moment would be similar to the one for the Ir^{4+} ion, where the latter can be thought as a $5d^1$ hole [39] (instead of $3d^1$ electron for V^{4+}). An interesting consequence of this correspondence is that, the rich physics due to the spin-orbit entanglement for iridates, such as Kitaev interaction [40] and/or highly anisotropic exchange [39], may be found among the 3d transition metal oxides like vanadates.

The orbital nature of the V^{4+} local moment is consistent with the presence of significant (anti-symmetric) DM interaction. Moreover, for the same reason, we expect that the symmetric pseudo-dipolar interaction should be present and equally important as the DM interaction. This may not effect certain topological properties of the magnon bands too much as these properties are topologically robust. Since the local moment is effective spin-1/2, the single-ion anisotropy should not be present. As for the universal long-distance property in the vicinity of the

transition, one does not need to worry too much about the detailed form of the interaction. Due to the orbital character of the local moment, the lattice symmetry directly acts on the effective spin components that effectively reduces the ferromagnetic order parameters from having an $O(3)$ symmetry to the cubic symmetry. From the Ginzburg-Landau symmetry analysis, we propose the following action to describe the behavior of $\text{Lu}_2\text{V}_2\text{O}_7$ near the transition,

$$\mathcal{L} = a|\mathbf{M}|^2 + b|\mathbf{M}|^4 + \lambda_c[(M^x)^4 + (M^y)^4 + (M^z)^4] + \dots, \quad (7)$$

where \mathbf{M} is the coarse-grained ferromagnetic order parameter, and “...” represents the higher-order terms neglected here. The first two terms are isotropic with $a \approx a'(T - T_c)$, $a' > 0$ and $b > 0$. They can describe the conventional ferromagnetic transition for $O(3)$ -type order parameter, belong to the 3D Heisenberg universality class. We include the cubic anisotropy of the $\text{Lu}_2\text{V}_2\text{O}_7$ system via λ_c and require $\lambda_c < 0$. This cubic anisotropy then favors the order parameter \mathbf{M} to be aligned with the $\langle 001 \rangle$ directions, which is consistent with the experimental observation [24]. For a small λ_c , the system should be found still in the Heisenberg universality class when T is above but not too close to T_c . When T is further tuned to T_c , one expects a crossover from the Heisenberg universality class to the cubic universality class [41]. We mention that the critical exponents belong to these two universality classes are very close, Table I thus difficult to be distinguished from each other in experiments. Recent results in literature give $\gamma = 1.3895$ for the Heisenberg class [42] and $\gamma = 1.390$ for the cubic class [38], which are indeed close to the experimental result $\gamma = 1.402$ obtained in this work. At $T < T_c$, the cubic symmetry is spontaneously broken. The system has chosen one of the $\langle 001 \rangle$ directions and the order parameter becomes Ising-like, leading the critical exponent β belong to the Ising universality class.

In summary, we have investigated the critical behavior of ferromagnetic pyrochlore $\text{Lu}_2\text{V}_2\text{O}_7$ based on the measurements of isothermal magnetization $M(H)$ around T_c . We found that the $\beta = 0.322$ at $T < T_c$ and $\gamma = 1.417$ at $T > T_c$ are close to the predicted values of 3D Ising and cubic universality classes, respectively. This makes $\text{Lu}_2\text{V}_2\text{O}_7$ a rare example in which the critical behaviors associated with a ferromagnetic transition belong to different universality classes. We have rationalized the observed criticality from the Ginzburg-Landau theory with the quartic cubic anisotropy that microscopically originates from the anti-symmetric DM interactions.

Acknowledgments.—This work is supported by the National Key R&D Program of China (Grant Nos. 2018YFA0305700, 2018YFA0305800, 2016YFA0301001, 2016YFA0300500), the National Natural Science Foundation of China (Grant Nos. 11574377, 11834016,

11874400), the Strategic Priority Research Program and Key Research Program of Frontier Sciences of the Chinese Academy of Sciences (Grant Nos. XDB25000000, XDB07020100 and QYZDB-SSW-SLH013). J.P.S. and Y.Y.J. acknowledge support from the China Postdoctoral Science Foundation and the Postdoctoral Innovative Talent program.

* These authors contributed equally to this work.

† Present address: Faculty of Science, Wuhan University of Science and Technology, Wuhan, Hubei 430062, China
ganchen.physics@gmail.com

‡ jgcheng@iphy.ac.cn

- [1] Jason S. Gardner, Michel J. P. Gingras, and John E. Greedan, “Magnetic pyrochlore oxides,” *Rev. Mod. Phys.* **82**, 53–107 (2010).
- [2] C. Castelnovo, R. Moessner, and S. L. Sondhi, “Magnetic monopoles in spin ice,” *Nature* **451**, 42–45 (2008).
- [3] Steven T. Bramwell and Michel J. P. Gingras, “Spin Ice State in Frustrated Magnetic Pyrochlore Materials,” *Science* **294**, 1495–1501 (2001).
- [4] Hamid R. Molavian, Michel J. P. Gingras, and Benjamin Canals, “Dynamically Induced Frustration as a Route to a Quantum Spin Ice State in $\text{Tb}_2\text{Ti}_2\text{O}_7$ via Virtual Crystal Field Excitations and Quantum Many-Body Effects,” *Phys. Rev. Lett.* **98**, 157204 (2007).
- [5] M J P Gingras and P A McClarty, “Quantum spin ice: a search for gapless quantum spin liquids in pyrochlore magnets,” *Reports on Progress in Physics* **77**, 056501 (2014).
- [6] Kate Ross, Lucile Savary, Bruce Gaulin, and Leon Balents, “Quantum Excitations in Quantum Spin Ice,” *Phys. Rev. X* **1**, 021002 (2011).
- [7] Michael Hermele, Matthew P. A. Fisher, and Leon Balents, “Pyrochlore photons: The $U(1)$ spin liquid in a $S = \frac{1}{2}$ three-dimensional frustrated magnet,” *Phys. Rev. B* **69**, 064404 (2004).
- [8] Lucile Savary and Leon Balents, “Coulombic Quantum Liquids in Spin-1/2 Pyrochlores,” *Phys. Rev. Lett.* **108**, 037202 (2012).
- [9] SungBin Lee, Shigeki Onoda, and Leon Balents, “Generic quantum spin ice,” *Phys. Rev. B* **86**, 104412 (2012).
- [10] Yi-Ping Huang, Gang Chen, and Michael Hermele, “Quantum Spin Ices and Topological Phases from Dipolar-Octupolar Doublets on the Pyrochlore Lattice,” *Phys. Rev. Lett.* **112**, 167203 (2014).
- [11] Lucile Savary, Kate A. Ross, Bruce D. Gaulin, Jacob P. C. Ruff, and Leon Balents, “Order by Quantum Disorder in $\text{Er}_2\text{Ti}_2\text{O}_7$,” *Phys. Rev. Lett.* **109**, 167201 (2012).
- [12] Alannah M. Hallas, Jonathan Gaudet, and Bruce D. Gaulin, “Experimental insights into ground-state selection of quantum xy pyrochlores,” *Annual Review of Condensed Matter Physics* **9**, 105–124 (2018).
- [13] Mathieu Taillefumier, Owen Benton, Han Yan, L. D. C. Jaubert, and Nic Shannon, “Competing Spin Liquids and Hidden Spin-Nematic Order in Spin Ice with Frustrated Transverse Exchange,” *Phys. Rev. X* **7**, 041057 (2017).

- [14] Nic Shannon, Karlo Penc, and Yukitoshi Motome, “Nematic, vector-multipole, and plateau-liquid states in the classical $O(3)$ pyrochlore antiferromagnet with bi-quadratic interactions in applied magnetic field,” *Phys. Rev. B* **81**, 184409 (2010).
- [15] Gang Chen, “Spectral periodicity of the spinon continuum in quantum spin ice,” *Phys. Rev. B* **96**, 085136 (2017).
- [16] Gang Chen, “Dirac’s “magnetic monopoles” in pyrochlore ice $u(1)$ spin liquids: Spectrum and classification,” *Phys. Rev. B* **96**, 195127 (2017).
- [17] Fei-Ye Li, Yao-Dong Li, Yong Baek Kim, Leon Balents, Yue Yu, and Gang Chen, “Weyl magnons in breathing pyrochlore antiferromagnets,” *Nature Communications* **7**, 12691 (2016).
- [18] Fei-Ye Li and Gang Chen, “Competing phases and topological excitations of spin-1 pyrochlore antiferromagnets,” *Phys. Rev. B* **98**, 045109 (2018).
- [19] Shao-Kai Jian and Wenxing Nie, “Weyl magnons in pyrochlore antiferromagnets with an all-in-all-out order,” *Phys. Rev. B* **97**, 115162 (2018).
- [20] G. V. Bazuev, A. A. Samokhalov, Y. N. Movozov, I. I. Matveenko, V. S. Babushkin, T. I. Arbuzova, and G. P. Shveikin, “Magnetic properties of hypovanadates of rare-earth elements having pyrochlorine structure,” *Sov. Phys. Solid State* **19**, 3274–3278 (1977).
- [21] Shin-ichi Shamoto, Takehito Nakano, Yasuo Nozue, and Tsuyoshi Kajitani, “Substitution effects on ferromagnetic Mott insulator $\text{Lu}_2\text{V}_2\text{O}_7$,” *Journal of Physics and Chemistry of Solids* **63**, 1047–1050 (2002).
- [22] Hirohiko Ichikawa, Luna Kano, Masahiro Saitoh, Shin Miyahara, Nobuo Furukawa, Jun Akimitsu, Tetsuya Yokoo, Takeshi Matsumura, Masayasu Takeda, and Kazuma Hirota, “Orbital ordering in ferromagnetic $\text{Lu}_2\text{V}_2\text{O}_7$,” *Journal of the Physical Society of Japan* **74**, 1020–1025 (2005).
- [23] Takashi Kiyama, Takahisa Shiraoka, Masayuki Itoh, Luna Kano, Hirohiko Ichikawa, and Jun Akimitsu, “Direct observation of the orbital state in $\text{Lu}_2\text{V}_2\text{O}_7$: A ^{51}V NMR study,” *Phys. Rev. B* **73**, 184422 (2006).
- [24] Y Onose, T Ideue, H Katsura, Y Shiomi, N Nagaosa, and Y Tokura, “Observation of the magnon Hall effect,” *Science* **329**, 297–299 (2010).
- [25] T. Ideue, Y. Onose, H. Katsura, Y. Shiomi, S. Ishiwata, N. Nagaosa, and Y. Tokura, “Effect of lattice geometry on magnon Hall effect in ferromagnetic insulators,” *Phys. Rev. B* **85**, 134411 (2012).
- [26] M. Mena, R. S. Perry, T. G. Perring, M. D. Le, S. Guerrero, M. Storni, D. T. Adroja, Ch. Rüegg, and D. F. McMorrow, “Spin-wave spectrum of the quantum ferromagnet on the pyrochlore lattice $\text{Lu}_2\text{V}_2\text{O}_7$,” *Phys. Rev. Lett.* **113**, 047202 (2014).
- [27] H. J. Xiang, E. J. Kan, M.-H. Whangbo, C. Lee, Su-Huai Wei, and X. G. Gong, “Single-ion anisotropy, Dzyaloshinskii-Moriya interaction, and negative magnetoresistance of the spin- $\frac{1}{2}$ pyrochlore $R_2\text{V}_2\text{O}_7$,” *Phys. Rev. B* **83**, 174402 (2011).
- [28] Ying Su, X. S. Wang, and X. R. Wang, “Magnonic Weyl semimetal and chiral anomaly in pyrochlore ferromagnets,” *Phys. Rev. B* **95**, 224403 (2017).
- [29] Alexander Mook, Jürgen Henk, and Ingrid Mertig, “Tunable magnon weyl points in ferromagnetic pyrochlores,” *Phys. Rev. Lett.* **117**, 157204 (2016).
- [30] H Eugene Stanley, *Introduction to phase transitions and critical phenomena* (Oxford University Press, Oxford, 1971).
- [31] S. N. Kaul, “Static critical phenomena in ferromagnets with quenched disorder,” *J. Mag. Mag. Mater.* **53**, 5 (1985).
- [32] H. D. Zhou, E. S. Choi, J. A. Souza, J. Lu, Y. Xin, L. L. Lumata, B. S. Conner, L. Balicas, J. S. Brooks, J. J. Neumeier, and C. R. Wiebe, “Magnetic-polaron-driven magnetoresistance in the pyrochlore $\text{Lu}_2\text{V}_2\text{O}_7$,” *Phys. Rev. B* **77**, 020411 (2008).
- [33] F. Y. Yang, C. L. Chien, X. W. Li, Gang Xiao, and A. Gupta, “Critical behavior of epitaxial half-metallic ferromagnetic CrO_2 films,” *Phys. Rev. B* **63**, 092403 (2001).
- [34] H. Yanagihara, Wesley Cheong, M. B. Salamon, Sh. Xu, and Y. Moritomo, “Critical behavior of single-crystal double perovskite $\text{Sr}_2\text{FeMoO}_6$,” *Phys. Rev. B* **65**, 092411 (2002).
- [35] James S. Kouvel and Michael E. Fisher, “Detailed magnetic behavior of nickel near its Curie point,” *Phys. Rev.* **136**, A1626–A1632 (1964).
- [36] B Widom, “Degree of the critical isotherm,” *The Journal of Chemical Physics* **41**, 1633–1634 (1964).
- [37] J.-G. Cheng, Y. Sui, J.-S. Zhou, J. B. Goodenough, and W. H. Su, “Transition from orbital liquid to Jahn-Teller insulator in orthorhombic perovskites $R\text{TiO}_3$,” *Phys. Rev. Lett.* **101**, 087205 (2008).
- [38] José Manuel Carmona, Andrea Pelissetto, and Ettore Vicari, “ N -component Ginzburg-Landau Hamiltonian with cubic anisotropy: A six-loop study,” *Phys. Rev. B* **61**, 15136–15151 (2000).
- [39] Gang Chen and Leon Balents, “Spin-orbit effects in $\text{Na}_4\text{Ir}_3\text{O}_8$: A hyper-kagome lattice antiferromagnet,” *Phys. Rev. B* **78**, 094403 (2008).
- [40] G. Jackeli and G. Khaliullin, “Mott Insulators in the Strong Spin-Orbit Coupling Limit: From Heisenberg to a Quantum Compass and Kitaev Models,” *Phys. Rev. Lett.* **102**, 017205 (2009).
- [41] Amnon Aharony, “Critical behavior of anisotropic cubic systems,” *Phys. Rev. B* **8**, 4270–4273 (1973).
- [42] Riccardo Guida and Jean Zinn-Justin, “Critical exponents of the N -vector model,” *Journal of Physics A: Mathematical and General* **31**, 8103 (1998).